JOURNAL OF GEOPHYSICAL RESEARCH, VOL. 112, D05212, doi:10.1029/2005JD006602, 2007

Nitric acid particles in cold thick ice clouds observed at global scale: Link with lightning, temperature, and upper tropospheric water vapor

H. Chepfer,[1] P. Minnis,[2] P. Dubuisson,[3] M. Chiriaco,[1] S. Sun-Mack,[4] and E. D. Rivière[5]

Received 19 August 2005; revised 16 January 2006; accepted 4 October 2006; published 14 March 2007.

[1] Signatures of nitric acid particles (NAP) in cold thick ice clouds have been derived from satellite observations. Most NAP are detected in the tropics (9 to 20% of clouds with T < 202.5 K). Higher occurrences were found in the rare midlatitudes very cold clouds. NAP occurrence increases as cloud temperature decreases, and NAP are more numerous in January than July. Comparisons of NAP and lightning distributions show that lightning seems to be the main source of the NO_x, which forms NAP in cold clouds over continents. Qualitative comparisons of NAP with upper tropospheric humidity distributions suggest that NAP may play a role in the dehydration of the upper troposphere when the tropopause is colder than 195 K.

Citation: Chepfer, H., P. Minnis, P. Dubuisson, M. Chiriaco, S. Sun-Mack, and E. D. Rivière (2007), Nitric acid particles in cold thick ice clouds observed at global scale: Link with lightning, temperature, and upper tropospheric water vapor, *J. Geophys. Res.*, *112*, D05212, doi:10.1029/2005JD006602.

1. Introduction

[2] Water vapor, the main atmospheric greenhouse gas [*Key et al.*, 2000], plays key role in climate change, especially when its effects in the upper troposphere are considered [*Intergovernmental Panel on Climate Change*, 2001; *Hartmann*, 2002]. Mean upper tropospheric humidity (UTH) has been anomalously decreasing over the entire tropics since 2001 [*Randel et al.*, 2004]. Dehydration of the upper troposphere (UT) over large areas in the tropics is linked to variations in the temperature of the tropical tropopause layer (TTL), particularly in the winter hemisphere [*Holton and Gettelman*, 2001; *Zhou et al.*, 2004] but the processes inducing the variations in UTH are not well understood. Ice clouds [*Liou*, 1986; *Stephens et al.*, 1990] are involved in the UT dehydration [*Hartmann et al.*, 2001; *Dessler and Sherwood*, 2003] serving as both sinks and sources of humidity. However, the factors governing the relative amounts of UT frozen and gaseous water are poorly understood. Recently, condensed phase HNO_3 particles were measured in situ within ice clouds at temperatures T between 197 and 224 K [*Popp et al.*, 2004] confirming the presence of nitric acid particles (NAP) near the tropical tropopause, a phenomenon that has been observed indirectly for some time [*Hamill and Fiocco*, 1988; *Omar and Gardner*, 2001; *Hervig and McHugh*, 2002; *Jensen and Drdla*, 2002]. Other in situ [*Gao et al.*, 2004] and model [*Kramer et al.*, 2006] studies demonstrated that UT nitric acid interacts with ice particles and modifies the UTH.

[3] In the other side nitric acid uptake on ice is uncertain [e.g., *Kramer et al.*, 2003], but if it occurs substantially in cirrus then it can make a very large contribution to the budget of HNO_3 via particle sedimentation/precipitation [e.g., *Lawrence and Crutzen*, 1998; *von Kuhlmann and Lawrence*, 2005], which in turn influences the amount of HNO3 available for the formation of particles.

[4] Satellite remote sensing is needed to better evaluate the role of HNO_3 in ice clouds and its impact on tropical UTH. Global distributions of NAP signatures in cold thick ice clouds derived from satellite data are shown here for the first time. They are used to show that lightning is probably the main source of NO_x (HNO_3 precursor) over land. It also shows that NAP occurs more frequently when the temperature is extremely low in the upper tropical troposphere. Qualitative comparison between NAP distributions, UT dehydration anomaly and TTL temperatures suggest that NAP could be involved in the UT dehydration in very cold regions.

2. Observations

2.1. Method

[5] In an attempt to explain radiance anomalies associated with ice cloud retrievals, a remote sensing technique was developed to detect the signature of nitric acid in ice clouds from satellite observations [*Chepfer et al.*, 2005]. Nitric acid is detected in thick cold ice clouds using brightness temperature differences (BTD) between the 11- and 12-μm radiances measured by satellite imagers. For pristine ice clouds and perfect satellite calibrations, the BTD will always be zero or positive because ice and water vapor are more absorptive at 12 than at 11 μm. Negative BTDs

[1] Laboratoire de Météorologie Dynamique/Institut Pierre-Simon Laplace, Ecole Polytechnique, Palaiseau, France.
[2] NASA Langley Research Center, Hampton, Virginia, USA.
[3] Laboratoire Écosystèmes Littoraux et Côtiers, Universitédu Littoral, Wimereux, France.
[4] Science Applications International Corporation, Hampton, Virginia, USA.
[5] Laboratoire de Physique et Chimie de l'Environnement, Centre National de la Recherche Scientifique/Université d'Orléans, Orléans, France.

0148-0227/07/2005JD006602$09.00

(NBTD) occur in the presence of nitric acid located in or above a thick cold ice cloud because HNO_3 has an 11-μm absorption band. The effect is only detectable when viewing a thick cold ice cloud, which acts as a blackbody that masks the upwelling radiances from under the cloud [*Chepfer et al.*, 2005]. This signature does not occur for optically thin ice clouds because BTDs for optically thin cirrus clouds are positive and any nitric acid that is present in those clouds would only make the BTDs less positive. Furthermore, NBTD can also be observed in radiances from dust storms [*Gu et al.*, 2003; *Sokolik*, 2002] as a result of the absorption characteristics of sand and volcanic ash aerosols. Selection of only thick high clouds precludes misidentification of aerosols as a nitric acid signal. Future work could identify some other component causing NBTD, but at this stage, nitric acid particles remain the best candidate in absence of dust.

[6] Moderate Resolution Imaging Spectroradiometer (MODIS [*King et al.*, 1996, 2003; *Platnick et al.*, 2003]) data collected from Terra and Aqua in January 2003 as well as from Aqua in July 2004 are used to examine the global distributions of NBTD in ice clouds. Cloudy pixels are identified as in the work by *Minnis et al.* [2003] as part of the Clouds and the Earth's Radiant Energy System cloud products. The uncertainty in brightness temperature measured by MODIS is nominally less than 0.05 K. To account for possible measurement biases for T_{11} < 230 K, NBTD distribution obtained in selecting NBTD < −0.2 K instead of NBTD < 0 are also studied.

2.2. Data Set

[7] Figures 1c and 1d show the number of cloud events with 11-μm brightness temperatures T_{11} < 202.5 K as a function of latitude, indicating that they occur mostly at low latitudes 30° around the ITZC (Intertropical Convergence Zone) located at 10°N in July and 5°S in January, and also in small quantities in the midlatitude winter hemisphere. There, the cloudy pixels may also be due to false cloud detection above snow surfaces, which are common at those latitudes in winter. There are naturally more cloud events occurring above sea surfaces than over land. No significant diurnal variation in frequency of occurrence is evident except during July above land, where more cold clouds occur at night than during the day. Cold clouds are slightly more numerous in January than during July. The only noticeable difference between the months is that the cold clouds over land are significantly greater in January in the tropics during the daytime. At high latitudes in the winter hemisphere, the scarcity of potential measurements during daytime precludes the use of the data for defining a diurnal cycle. Hence data corresponding to latitudes poleward of 60°N in January and 50°S in July are not considered in the following discussion.

[8] The number of cloud events when T_{11} < 230 K (Figures 1a and 1b, solid lines) is large at nearly all latitudes. The event frequencies have quite similar characteristics in January and July with a relative minimum in the winter hemisphere at a distance of 30° of latitude from the ITCZ (−20° in Figure 1a and +20° in Figure 1b).

[9] Very cold clouds with T_{11} < 195 K (Figure 1e) occur relatively frequently around the ITCZ with more cold clouds during the night over ocean and more above ocean than over land surfaces. Very cold clouds are more abundant in January than in July as expected given the seasonal tropopause temperature variations along the ITCZ [*Zhou et al.*, 2004]. The diurnal variations above ocean are similar during the two months, but different above land. Convection over Brazil and sub-Saharan Africa causes a significant increase in daytime clouds over land during January.

2.3. Spatial Distribution of NAP Signatures

[10] In terms of sheer numbers, NAP (Nitric Acid Particles) signatures are more common in clouds over ocean than those over land and they are seasonally (January/July) invariant: More than 40 and 21% of NAP occurs during night and day, respectively, over ocean (Table 1a). Over land, the daytime contribution weights 21% of the total in January whereas it only weights 13.5% of the total amount of NAP in July.

[11] The distributions of NAP for cold clouds (Figure 2) correspond to the main convective areas and to a few areas off the Antarctic coast during July that are likely associated with polar stratospheric clouds [*Voigt et al.*, 2000]. The relative occurrence of NAP for T_{11} < 202.5 K is relatively constant at about 17–20% around the ITCZ over land and ocean during both months (Figures 3a and 3b). Moreover there is a persistent asymmetry between the two hemispheres above ocean, with a larger NAP frequency peak in the northern midlatitudes. The maxima, located around 40° north and south of the ITCZ, reach values between 60 and 100%. Although the extremely cold clouds are less frequent in the midlatitudes (Figures 1a and 1b), when they occur there, they are more often associated (30 to 80%) with NAPs than when they occur in the tropics.

[12] NAPs in warmer clouds (T_{11} < 230 K) follow a pattern similar to those in cold clouds but are less frequent overall (Figures 3c and 3d). NAP occur in the ITCZ area in only 5% of the tropical ice clouds indicating that their occurrence frequency mainly depends on cloud temperature. Relative maxima for those warmer ice clouds occur in January at 30°N over ocean at night, 30°S (Argentina/Africa) during the day, and 75°N (Greenland/Siberia) during the night. Those features are confirmed in the global means (Table 1c). For a constant cloud amount, the production of NAP is greater above ocean during the night than during the day and than above land at any time.

[13] To account for possible measurement biases for T_{11} < 230 K, Figure 3e and Table 1c show the NAP distribution obtained in selecting NBTD < −0.2 K instead of NBTD < 0. This precaution to avoid overestimation of NAP signatures in ice clouds reduces the occurrence frequency by a factor of two. Typically 5 to 15% of clouds with T_{11} < 202.5 K around the ITCZ have NBTD < −0.2 K and over ocean at night NBTD < −0.2 K in only 10% of cases compared to 22% for NBTD < 0.0 K (Table 1c).

[14] The low percentage of NAP in ice clouds associated with large brightness temperatures (Figure 3e) can be interpreted as an effective decrease of the condensed nitric acid concentration within the cloud or as a decrease of the cloud opacity, which leads to a smaller contrast between the two channels (11 and 12 μm) for the same condensed nitric acid concentration. It follows that the nitric acid condensates in ice clouds will be underestimated for nonopaque

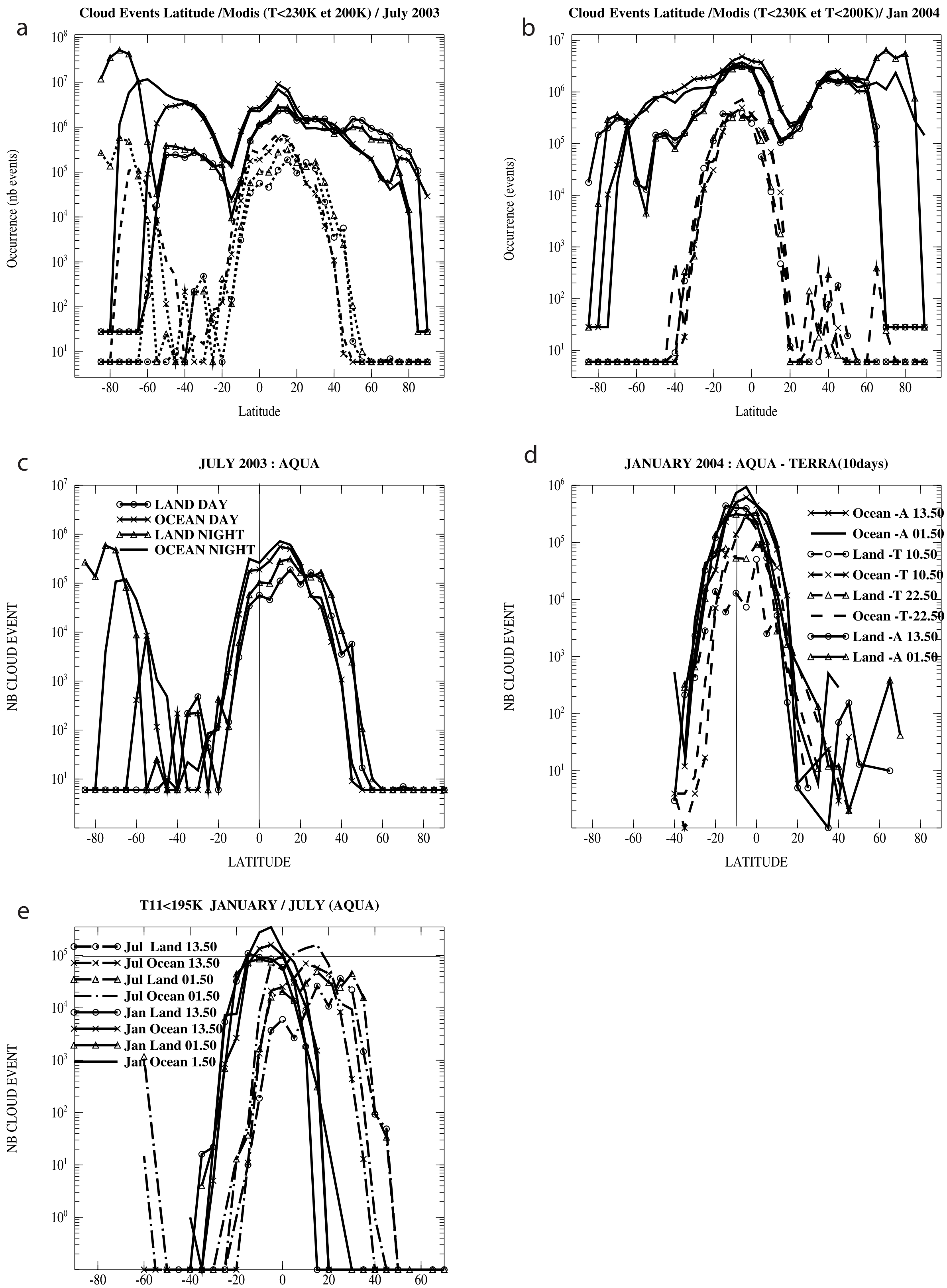

Figure 1. Number of cloudy pixels as a function of latitude. (a and b) T_{11} < 230 K (solid line), T_{11} < 202.5 K (dashed line), MODIS/Aqua, July/January. (c and d) T_{11} < 202.5 K, July (Aqua), January (Aqua and Terra). (e) T_{11} < 195 K, Aqua, January/July.

Table 1a. Distribution of the NAP Signatures All Over the Globe (Except Very High Latitudes) for Cloud Brightness Temperature at 11 μm (T_{11}) < 202.5 K[a]

	January	July
Total Nb of NAP pixels	1548833	1448133 (−7%)
Ocean, day	21%	22.5%
Land, day	21% (strong increase South America)	13.5%
Ocean, night	41%	45.5%
Land, night	17%	20%

[a]NAP are detected in thick cold ice clouds using negative brightness temperature differences (NBTD) between the 11- and 12-μm radiances measured by Moderate Resolution Imaging Spectroradiometer (MODIS) (18).

clouds, and the statistical results (Figure 3) should be considered as possibly underestimating NAP frequencies.

2.4. Time Variation

2.4.1. Diurnal Cycle

[15] The NAP occurrence frequency varies as a function of local time (LT) in a similar fashion at all latitudes over a range of temperatures (Figure 4). The diurnal cycle amplitude decreases with increasing temperature, further supporting the idea that NAP is more common at lower temperatures. During daytime (1030 and 1330 LT), NAP occur more frequently above land than over ocean at all cloud temperatures, possibly as a result of stronger convection over land [*LeMone and Zipser*, 1980]. The opposite occurs at 0130 LT when convection is reduced over most land areas. Over water, NAP signatures are more common at night than during the day, on average (Figure 4 and Table 1c). Conversely, there is no clear mean diurnal cycle over land (Figure 4 and Table 1c) despite some sharp day/night contrasts in specific regions such as the southern midlatitudes (Figures 2c and 2d). The frequency of the NAP signature is strongly variable with time during the day when the threshold is reduced (Figure 5b). Nevertheless, the diurnal cycle presented here (Figure 4) is built in using data collected by two different satellites, so that it may also be simply due to an artifact in the intercalibration between the two instruments. It is hence difficult to draw firm physical conclusion from this diurnal cycle.

2.4.2. Monthly Variation

[16] NAPs occur more often in January than in July (Tables 1a and 1b). Considering all ice clouds with T_{11} < 230 K, the NAP frequency is 17.6% higher in January than in July (Table 1b). This increase is mainly due to NAPs associated with T_{11} between 220 and 230 K occurring over Greenland and Siberia (70°N, Figure 3d) during the winter night. These polar signatures are likely produced by NAP contained in PSCs located above very cold surfaces [*Voigt et al.*, 2000]. Considering clouds with T_{11} < 202.5 K (tropical clouds, Figure 1b), the global NAP occurrence increases by 7% between July and January (Table 1a). This rise is partly due to more frequent NAPs over land during the day along the ITCZ near Brazil and south central Africa (Figure 2). Since the percentage of NAP occurrence is the same for both months (Table 1), this increase is mainly induced by more cold clouds in those regions (Figure 1e) because of convection. The equivalent amount of cold clouds is not evident over Northern Hemisphere land surfaces in July.

2.5. Temperature Dependency

[17] The distributions in Figure 2 are typical of other T_{11} and NAP ranges where the proportion of NAPs increases at lower temperatures. Figures 5a and 5b confirm that NAP frequency decreases with increasing cloud temperature with a maximum of 32% (25%) for T_{11} < 195 K. The slope of this variation is nearly the same for all cases, but increases for T_{11} < 195 K. For clouds with T_{11} < 210 K and for

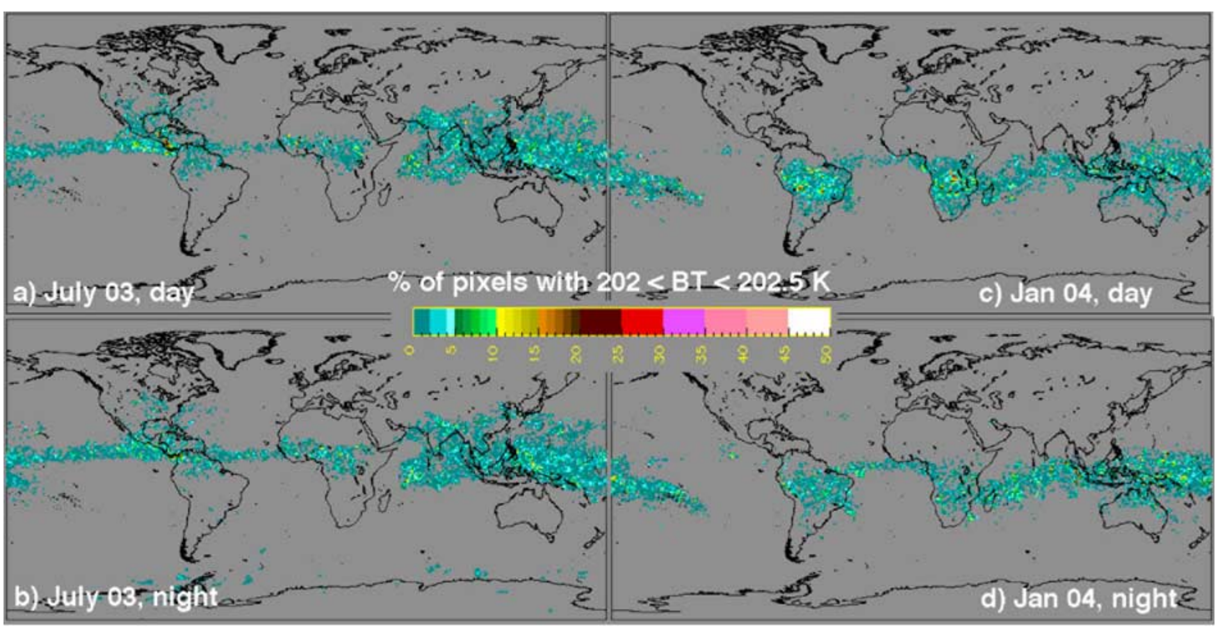

Figure 2. NAP frequencies in cloudy pixels with T_{11} between 202 and 202.5 K with NBTD between 0 and −0.5 K from MODIS/Aqua. July 2003 (a) during the day and (b) during the night. January 2004 (c) during the day and (d) during the night.

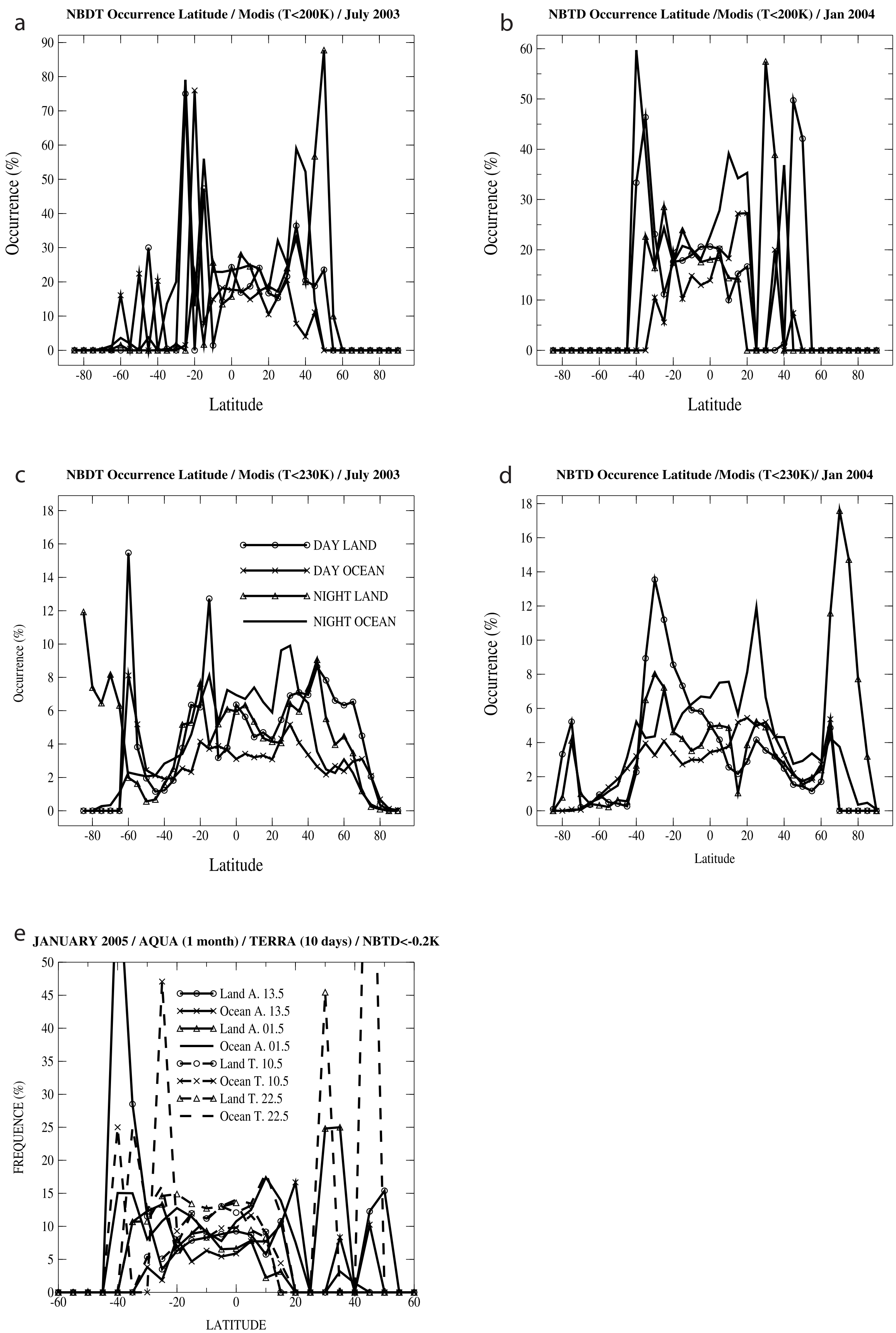

Figure 3. NAP frequencies as a function of latitude from MODIS/Aqua. For clouds with $T_{11} < 202.5$ K in (a) July 2003 and (b) January 2004. For clouds with $T_{11} < 230$ K in (c) July 2003 and (d) January 2004. (e) Same as Figure 1b but assuming a -0.2 K bias on NBTD measured by MODIS (NBTD < -0.2 K).

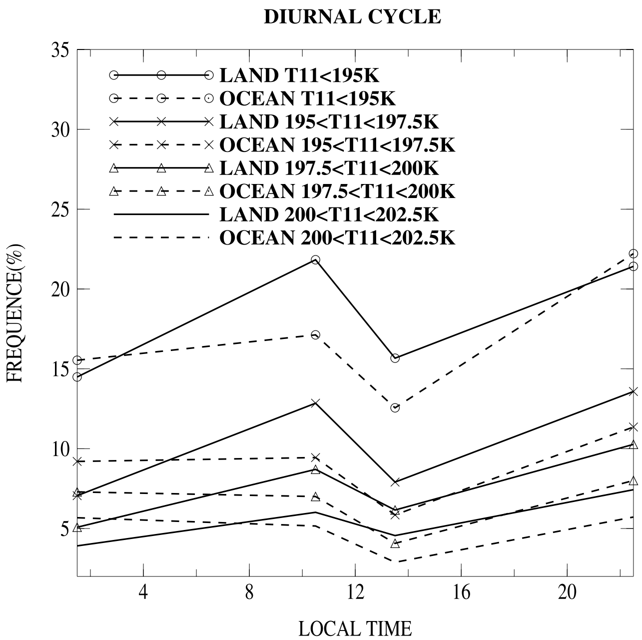

Figure 4. Diurnal cycle of NAP frequencies from MODIS/Aqua (1330 and 0130 LT) and Terra (1030 and 2230 LT) for clouds with $T_{11} < 202.5$ K in January 2003 (NBTD < -0.2 K).

constant values of T_{11}, NAP are less frequent in January than in July at all times of day over all surfaces (Figure 5a) independent of the cloud amount. Despite a consistent increase of NAP occurrence as temperature decreases, the frequency can vary by a factor of two at a constant temperature depending on the time of day (Figure 5b).

3. Discussion

[18] Two different categories of ice clouds containing NAP are evident in the results: very cold ice clouds ($T_{11} <$ 202.5 K) resulting from convection around the ITCZ, and midlatitude or polar (PSCs) ice clouds that can have higher temperatures ($202.5 < T_{11} < 230$ K) but more frequently (30 to 70%) produce NAP than the tropical clouds. Of the ITCZ clouds, nearly 20% (or 9%, Table 1c) contain nearly constant signatures of NAP.

[19] NAP can consist in Nitric Acid Trihydrate particles (NAT [*Hanson and Mauersberger*, 1988; *Wornsop et al.*, 1993; *Toon et al.*, 1994]) or Δ-ice particles (NAT adsorbed on ice crystal [*Gao et al.*, 2004]). Both of them contain HNO_3 and H_2O ($HNO_3.3H_2O$). Passive remote sensing cannot distinguish between tenuous NAT cloud layer located slightly above (lower temperature) the convective cloud and Δ-ice particle located at warmer temperatures at the top of the convective cloud itself. Possible links between spatio-temporal distributions of NAP signatures and HNO_3 precursors as well as UTH are discussed hereafter.

3.1. Origin of HNO_3

[20] HNO_3 occurs in significant amounts in the lower troposphere, but because of its high solubility it is scavenged by convective clouds [*Giorgi and Chameides*, 1986; *Crutzen and Lawrence*, 2000], and can hardly be transported into the tropical UT. Hence HNO_3 occurring in the tropical UT is produced at high altitudes by oxidation of NO_2 ($NO_2 + OH{+}M \rightarrow HNO_3 + M$, M being a molecule of air). OH is formed during daytime as a result of photodissociation and can be consumed by oxidation reaction. NO_2 is naturally produced by lightning all over the globe and generated from anthropogenic sources like fossil fuel burning that produces NO_x (not soluble), which can be transported to the UT. The amount of HNO_3 available for formation of NAP in the tropical UT will result of a competition between two processes: an increased amount of HNO_3 precursor (NO_2) by lightning or anthropogenic sources and the scavenging of HNO_3 by convective clouds. Increased NAP occurrences (Figure 2) are not observed in cold ice clouds over fossil fuel burning areas (e.g., eastern China coast, US, northern Europe), but NAP (Figure 2) and lightning (Figures 6a and 6b) locations coincide over South America, sub-Saharan Africa, and Australia in January, and over the Sahel and Himalayas in July, as well as over the main marine convective areas. Those similarities suggest that lightning is the main source of NO_x in the production of HNO_3 and hence NAP. Because of typically stronger convection over land, lightning occurs more frequently over land than over oceans [*Boccipio et al.*, 2000]. The land-ocean contrast is very strong during the day with the 1600 LT lightning maximum [*Williams et al.*, 2000] being nearly four times greater than over ocean. At other times though, the land-sea contrast is very small. Even though all satellite overpasses occur at times off this maximum lightning peak, NAP signatures present a land-ocean contrast during the day (Figure 5) that is consistent with lightning variation.

3.1.1. Ocean

[21] In the ±20° latitude belt, lightning occurs most often over the tropical western Pacific (TWP, Figures 6a and 6b) and Indian oceans where there is a high frequency of NAP signatures (Figure 3).

3.1.2. Land

[22] Most of the lightning regions included in the ±20° latitude bands are consistent with the NAP signatures (Figures 2 and 6a–6b). At 30°S, other important land regions with heavy lightning, such as Argentina, South Africa and southern Australia (Figures 6a and 6b) contribute little to NAP occurrence in winter because the lightning is not associated with very cold clouds (Figures 1b–1d). Nevertheless, warmer clouds (230 K > T > 202.5 K) located in those regions can lead to a sharp NAP occurrence peak such as that at 30°S (Figure 3d), which effectively corresponds to those active lightning areas. Similar correspondence appears in summer, as most of the lightning contribution occurs in the southern US where clouds with $T_{11} < 202.5$ K occur less frequently. Those around 30°N (Figure 3a) are associated with the Himalayas where both lightning and NAP signatures occur consistently. Direct comparison between NAP and lightning diurnal cycles averaged over the globe is not pertinent, because it is biased by cloud temperatures. Nevertheless, comparisons in specific lightning regions such as Brazil or sub-Saharan Africa in January reveal more NAP during the day (Figure 2) consistent with the lightning patterns.

3.2. Link With UTH

[23] NAP takes the form of NAT at very low temperatures (typically T < 195 K) and Δ-ice particles (HNO_3 adsorbed

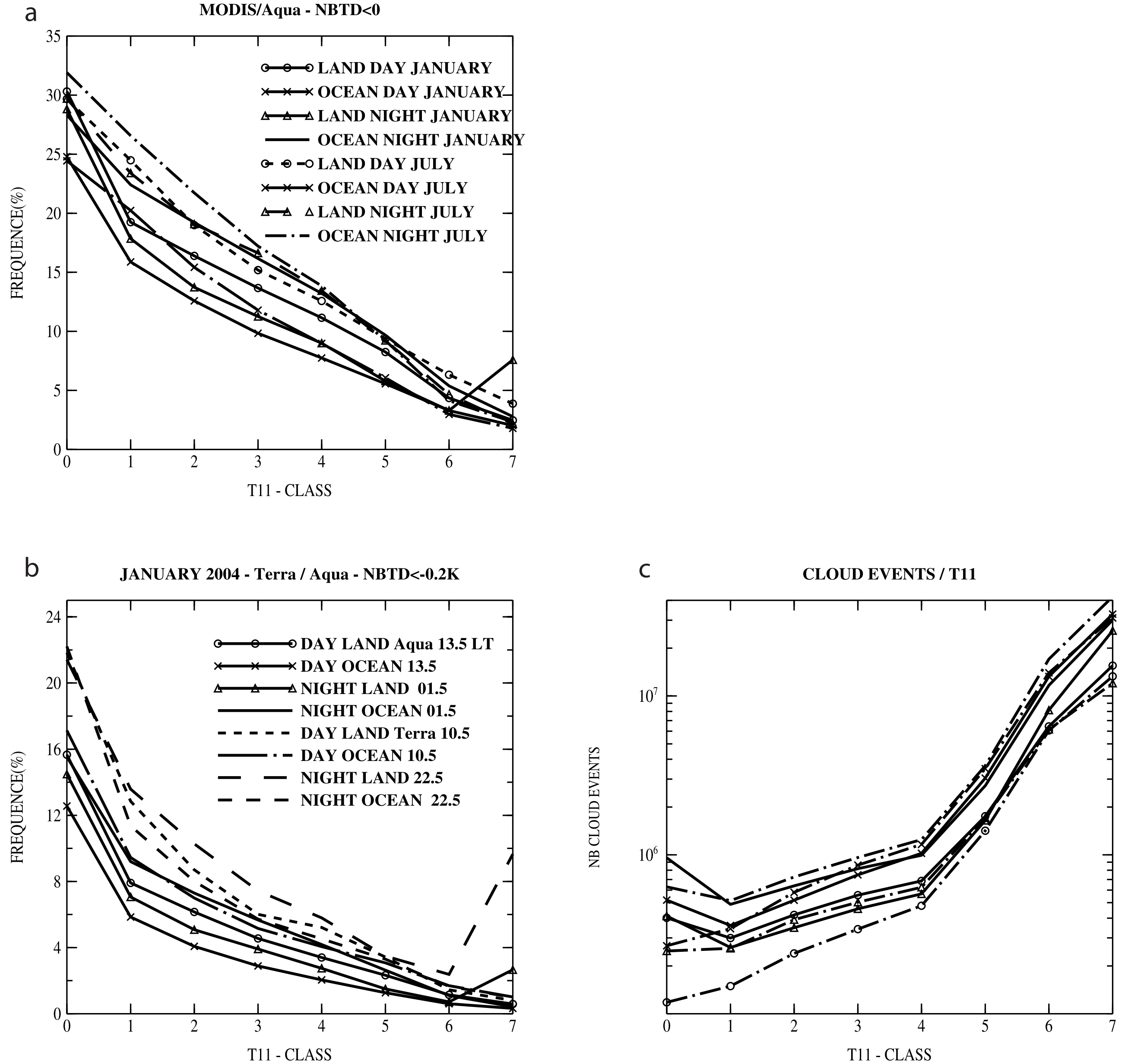

Figure 5. (a) NAP frequencies as a function of T_{11} from MODIS/Aqua in July and January. In the *x* axis, classes 0 to 7 correspond to T_{11} (<195 K), (195–197.5), (197.5–200), (200–202.5), (202.5–205), (205–210), (210–220), and (220–230). (b) NAP frequencies as a function of T_{11}. Same as Figure 5a but for NBTD < −0.2 K in January only including MODIS/Aqua and Terra data. (c) Number of cloud events as a function of T_{11} in January and July from MODIS/Aqua. January (solid line) and July (dashed line).

on ice crystal surface) at higher temperatures (224 > T > 195 K). In both temperature regimes, a change in UTH or an increase in NO_x concentration can alter the number of NAP particles, consequently pure NAT and Δ-ice particles interact with water vapor and could affect the UTH balance. Pure NAT particles will consume water vapor but formation of Δ-ice particles could cause an enhancement of UTH [*Gao et al.*, 2004].

Table 1b. Same as for T_{11} < 230 K

	January	July
Total Nb of NAP pixels	8013279	6812378 (−17.6%)
Ocean, day	21%	23.5%
Land, day	15%	18.5%
Ocean, night	33%	42%
Land, night	31% (strong increase Groenland/Siberia 220 K < BT-11 < 230 K)	16%

Table 1c. Average Percentage of NAP Signatures in Ice Clouds All Over the Globe[a]

	January	July
Ocean, day	15% (6%)	16%
Land, day	19% (8%)	20%
Ocean, night	22% (10%)	23%
Land, night	18% (8%)	21%

[a]Values given in parentheses assume −0.2 K bias on NBTD measured by MODIS.

[24] Global-scale UTH observations are available only from satellite data and correspond to a broad layer in the upper troposphere (200–500 hPa) in cloud free areas [*Tian et al.*, 2004; *Williams et al.*, 2000]. Thus comparisons of UTH with NAP occurrences observed only in presence of high clouds can only be qualitative, at best. Global maps of UTH [*Tian et al.*, 2004, Figure 4], lightning (Figures 6a and 6b) and NAPs (Figure 2) show evident correlation between the spatial distribution of these three variables in July, with maximum occurrence in the convective areas. UTH reaches a maximum at midnight over ocean and at 0300 LT over land, where the amplitude of the diurnal cycle is significantly larger [*Tian et al.*, 2004]. Consistently, NAP frequencies over ocean peak during the night (Figure 4). Above land, the spatial variation of UTH is well correlated with lightning and NAP, but the diurnal cycle is not. That is possibly due the fact that, the lightning maximum (1600 LT) is followed by the maximum deep convective cloudiness (1900 LT [*Tian et al.*, 2004]) that scavenged HNO_3 before the maximum UTH occurs (0300 LT [*Tian et al.*, 2004]). This phenomenon does not occur above ocean because the maximum deep convective cloud occurs later, 0900 LT the following day [*Tian et al.*, 2004].

[25] For a constant cloud temperature, NAP occurrence is larger in July than January independent of the cloud amount and the surface type (Figure 5). This can be explained by the greater humidity available in July [*Zhou et al.*, 2004] to produce NAP.

3.3. Link With Temperature

[26] Temperature plays a key role in the process because, for a given quantity of water vapor and HNO_3 in the UT, lower temperatures can lead to a slight decrease in UTH through the creation of NAT while warmer clouds can cause a slight increase in UTH through the creation of Δ-ice [*Gao et al.*, 2004]. The NAP occurrence clearly increases when temperature decreases (Figure 5b) and shows a discontinuity at T < 195 K (the NAT formation temperature in tropical conditions). Over ocean, the amount of HNO_3 precursor is quite stable in time when considering lightning as the dominant source of NO_x (no strong lightning diurnal cycle above ocean [*Williams et al.*, 2000], the amplitude of the UTH diurnal cycle is significantly less than over land [*Tian et al.*, 2004], and the cloud amount (T_{11} < 202.5 K) is nearly constant. Hence a change in the TTL temperature can

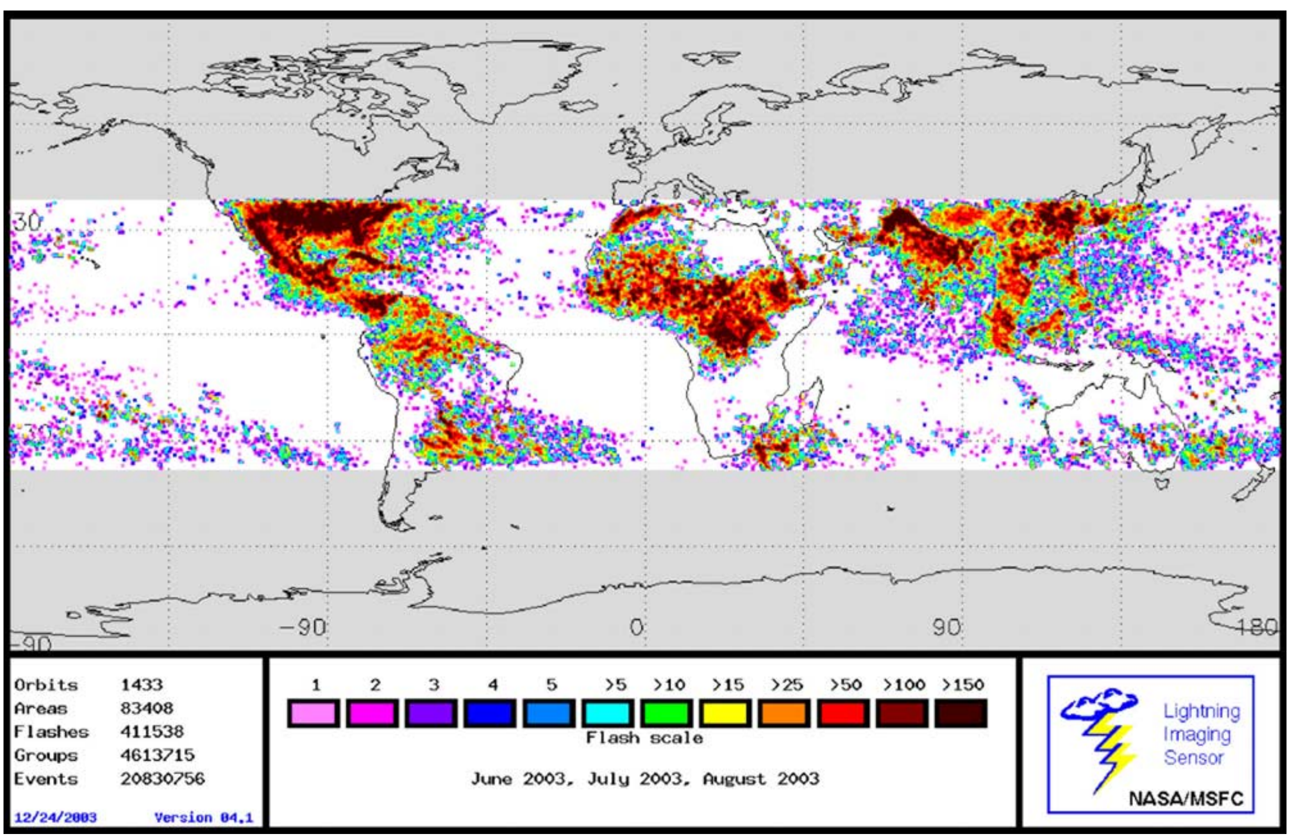

Figure 6a. Lightning flashes measured by LIS on board Tropical Rainfall Monitoring Measurements (TRMM) satellite during summer 2003. TRMM precesses through all times of day over a 45-day period. The lightning flashes measured therefore are diurnal averages including both high and low convective activity times. Courtesy of NASA/MSFC.

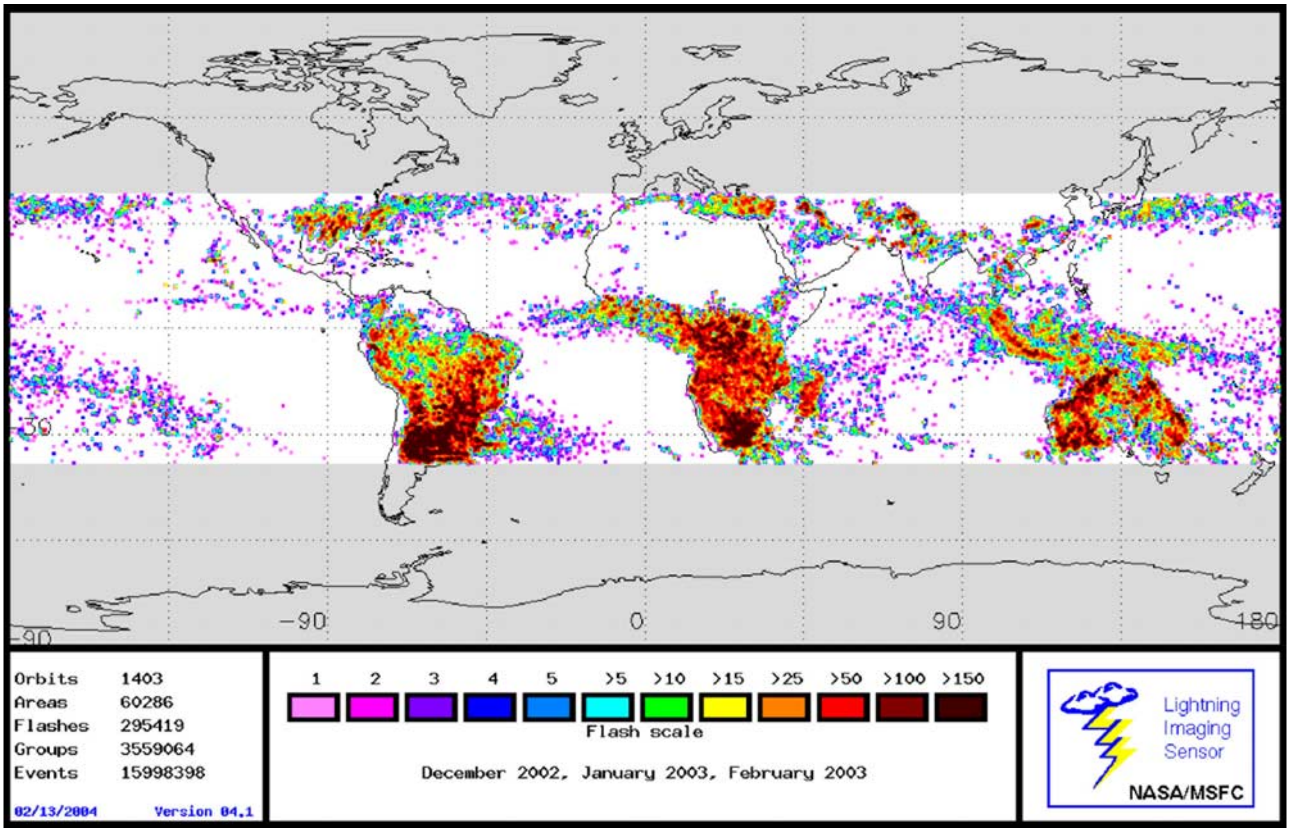

Figure 6b. Lightning flashes measured by LIS on board Tropical Rainfall Monitoring Measurements (TRMM) satellite during winter 2004. Courtesy of NASA/MSFC.

directly amplify or reduce the creation of NAT, and so reduce or increase the UTH.

[27] On average, the mean frequency of NAP in cold ice clouds (T_{11} < 202.5 K) is higher in January than in July (+7%), which is consistent with the lower January TTL temperature, leading to more clouds with T_{11} < 195 K (Figures 1e and 5c) and consequently to a higher contribution of those clouds to the total number of NAP signatures (Figure 7). The other cold clouds with 195 < T_{11} < 202.5 K are less efficient in producing NAP (Figures 5a and 5b), but are more numerous (Figure 5c) resulting in a significant contribution to the total number of occurrences (Figure 7). Their contribution to NAP formation is very strong in July when the UTH is higher. At those temperatures, NAP help maintain the relatively high UTH. For a constant temperature, more NAP is produced because more water vapor is available, but because NAP forms in Δ-ice particles at those temperatures, the UTH is enhanced [*Gao et al.*, 2004] and, therefore, UTH remains higher in July. During January, because of the lower tropopause temperature, the clouds are colder, producing more NAP particles with a larger proportion of NAT (T_{11} < 195 K in Figure 7) that consume UTH and tend to dehydrate the UT. The possible role of these NAP processes in the UTH regulation is supported by the fact that most NAP signatures occur over ocean with large contributions over the TWP and Indian Ocean. Those regions have very cold TTL temperatures, typically 200–196 K in July, with a significant seasonal variation leading to a cooling (195–190 K) in January [*Zhou et al.*, 2004] that is correlated to an unexplained decrease in UTH. The high

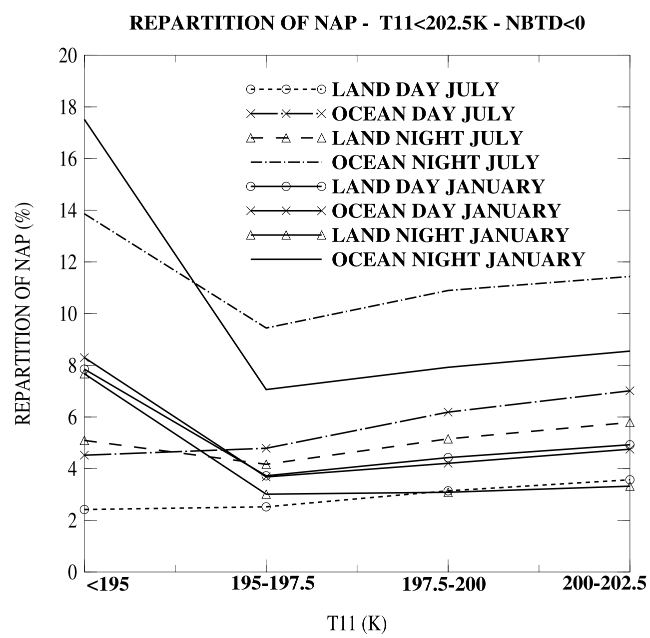

Figure 7. Distribution of the total NAP amount in cold clouds (T_{11} < 202.5 K) above land and ocean as a function of T_{11} in January and July from MODIS/Aqua. That is, 14% of the NAP signatures observed in July occur over ocean during the night in clouds with T_{11} < 195 K.

frequency of NAP observed in this region and the differences in the NAP formation processes occurring at the threshold of 195 K (Figure 5b) indicate that creation of NAT particles in the ice cloud tops is a process involved in the dehydration anomaly. The same process could also help explain the global decrease in UTH associated with a TTL temperature anomaly (-2 to -3 K) under progress since 2001 [*Randel et al.*, 2004]. For constant ice cloud ocean coverage and lightning occurrence, a drop in temperature by a few degrees makes the NAT creation process nearly twice as efficient when the barrier of 195 K is reached (Figure 5b). The UTH enhancement due to Δ-ice particles, then, would not be sufficient to compensate the UTH consumed by the relatively dense NAT, which precipitate more quickly than ice particles of similar volume, and the UT would be dehydrated.

4. Conclusion

[28] The January and July data sets indicate the presence of NAP in 20% (or 9% depending of the bias in the measurements) of cold clouds associated to $T_{11} < 202.5$ K in the tropics, and even more often in the midlatitudes: 30 to 80% of the clouds associated to $T_{11} < 230$ K. A majority of NAP signatures occur above tropical oceans. Lightning is a major source of NO_x for formation of NAP in the upper troposphere. Comparison between NAP frequency, cloud temperature, and UTH indicate that two regimes of NAP formation coexist. When $T_{11} < 195$ K, a large amount of NAT particles form and consume water vapor, but when $T_{11} > 195$ K, fewer NAT particles form while Δ-ice particles become more common and enhance the UTH. In January, the NAT are more frequent than in July because the ITCZ TTL is colder than 195 K, hence more extremely cold clouds ($T < 195$ K) form, and the NAP particles take the form of NAT, dehydrating the upper troposphere. In July, the TTL temperature exceeds 195 K causing most of the NAP to take the form of Δ-ice particles that help maintain the upper troposphere humidity. This process could explain part of the dehydration anomaly observed in the TWP with the decrease in TTL temperature being the driving force. It could also be a process involved in the UT dehydration observed over 5 years [*Randel et al.*, 2004]. Nevertheless, the data set considered here (two months only) does not allow to draw definitive conclusion on the seasonal variability, as for example over the Pacific Warm Pool and Indian Ocean, an El Nino January may differ from a La Nina January by as much as each differs from July. It is not possible from the current results to quantify the relative proportions and total impact of the two NAP formation processes in the upper troposphere dehydration: Are NAP particles the primary or an anecdotal process leading to upper tropical troposphere dehydration?

[29] The results obtained in this paper are based on the fact that NBTD are caused by the presence of NAP. Future work may show that other yet-to-be-identified component could also lead to NBTD, so that only part of the signatures analyzed here are due to NAP.

[30] **Acknowledgments.** The CERES MODIS analyses were supported by the NASA Earth Sciences Program through the CERES Project. The authors would like to thank the LIS science team for making available the lightning data.

References

Boccipio, D. J., S. Goodman, and S. Heckman (2000), Regional differences in tropical lightning distributions, *J. Appl. Meteorol.*, *39*, 2231–2248.

Chepfer, H., P. Dubuisson, M. Chiriaco, P. Minnis, S. Sun-Mack, and E. Rivière (2005), On the negative brightness temperature differences observed by satellites above thick ice clouds in the tropics, *Eos Trans. AGU*, *86*(18), Jt. Assem. Suppl., Abstract A13A-14.

Crutzen, P. J., and M. G. Lawrence (2000), The impact of precipitation scavenging on the transport of trace gases: A 3-dimensional model sensitivity study, *J. Atmos. Chem*, *37*, 81–112.

Dessler, A. E., and S. C. Sherwood (2003), A model of HDO in the tropical tropopause layer, *Atmos. Chem. Phys.*, *3*, 4489–4501.

Gao, R.-S., et al. (2004), Evidence that nitric acid increases relative humidity in low-temperature cirrus clouds, *Science*, *303*, 516–520.

Giorgi, F., and W. Chameides (1986), Rainout lifetimes of highly soluble aerosols and gases as inferred from simulations with a general circulation model, *J. Geophys. Res.*, *91*, 14,367–14,376.

Gu, Y., W. I. Rose, and G. J. S. Bluth (2003), Retrieval of mass and sizes of particles in sandstorms using two MODIS IR bands: A case study of April 7, 2001 sandstorm in China, *Geophys. Res. Lett.*, *30*(15), 1805, doi:10.1029/2003GL017405.

Hamill, P., and G. Fiocco (1988), Nitric acid aerosols at the tropical tropopause, *Geophys. Res. Lett.*, *15*(11), 1189–1192.

Hanson, D., and K. Mauersberger (1988), Laboratory studies of the nitric acid trihydrate: Implications for the south polar stratosphere, *Geophys. Res. Lett.*, *15*(8), 855–858.

Hartmann, D. L. (2002), Tropical surprises, *Science*, *295*, 811–812.

Hartmann, D. L., J. R. Holton, and Q. Fu (2001), The heat balance of the tropical tropopause, cirrus and stratospheric dehydration, *Geophys. Res. Lett.*, *28*, 1969–1972.

Hervig, M., and M. McHugh (2002), Tropical nitric acid clouds, *Geophys. Res. Lett.*, *29*(7), 1125, doi:10.1029/2001GL014271.

Holton, J. R., and A. Gettelman (2001), Horizontal transport and the dehydration of the stratosphere, *Geophys. Res. Lett.*, *28*, 2799–2802.

Intergovernmental Panel on Climate Change (2001), *Climate Change 2001: The Scientific Basis. Contribution of Working Group 1 to the Third Assessment Report*, edited by J. T. Houghton et al., 881 pp., Cambridge Univ. Press, New York.

Jensen, E., and K. Drdla (2002), Nitric acid concentrations near the tropical tropopause: Implications for the properties of tropical nitric acid trihydrate clouds, *Geophys. Res. Lett.*, *29*(20), 2001, doi:10.1029/2002GL015190.

Key, D., J. M. Russell III, and C. Philips (Eds.) (2000), SPARC Assessment of Upper Tropospheric and Stratospheric Water Vapour, *SPARC Report No. 2*, World Climate Research Programme, World Meteorological Organisation, Geneva. (Available at http://www.aero.jussieu.fr/~sparc/WAVASFINAL_000206/WWW_wavas/Cover.html).

King, M. D., et al. (1996), Airborne scanning spectrometer for remote sensing of cloud, aerosol, water vapour, and surface properties, *J. Atmos. Oceanic Technol.*, *13*, 777–794.

King, M. D., W. P. Menzel, Y. J. Kaufman, D. Tanre, B. C. Gao, S. Platnick, S. A. Ackerman, L. A. Remer, R. Pincus, and P. A. Hubanks (2003), Cloud and aerosol properties, precipitable water, and profiles of temperature and humidity from MODIS, *IEEE Trans. Geosci. Remote Sens.*, *41*, 442–458.

Kramer, M., et al. (2003), Nitric acid partitioning in cirrus clouds: A synopsis based on field, laboratory and model studies, *Atmos. Chem. Phys. Disc.*, *3*, 413–443.

Kramer, M., C. Schiller, H. Ziereis, J. Ovarlez, and H. Bunz (2006), Nitric acid partitioning in cirrus clouds: The role of aerosol particles and relative humidity, *Tellus, Ser. B*, *58*, 141–147.

Lawrence, M. G., and P. J. Crutzen (1998), The impact of cloud particle gravitational settling on soluble trace gas distributions, *Tellus, Ser. B*, *50*, 263–289.

LeMone, M. A., and E. J. Zipser (1980), Cumulonimbus vertical velocity events in GATE. Part I: Diameter, intensity, and mass flux, *J. Atmos. Sci.*, *37*, 2444–2457.

Liou, K. N. (1986), Review. Influence of cirrus clouds on weather and climate processes: A global perspective, *Mon. Weather Rev.*, *114*, 1167–1199.

Minnis, P., D. F. Young, S. Sun-Mack, P. W. Heck, D. R. Doelling, and Q. Z. Trepte (2003), CERES cloud property retrievals from imagers on TRMM, Terra, and Aqua, *SPIE 10th International Symposium on Remote Sensing, Conference on Remote Sensing, Clouds and Atmosphere*, pp. 37–48, edited by K. P. Shaefer et al., Int. Soc. for Opt. Eng., Bellingham, Wash.

Omar, A. H., and C. S. Gardner (2001), Observations by the lidar in space technology Experiment (LITE) of high-altitude cirrus clouds over the equator in regions exhibiting extremely cold temperatures, *J. Geophys. Res.*, *106*, 1227–1236.

Platnick, S., M. D. King, S. A. Ackerman, W. P. Menzel, B. A. Baum, J. C. Riedi, and R. A. Frey (2003), The MODIS cloud products: Algorithms and examples from Terra, *IEEE Trans. Geosci. Remote Sens.*, *41*, 459–473.

Popp, P. J., et al. (2004), Nitric acid uptake on subtropical cirrus cloud particles, *J. Geophys. Res.*, *109*, D06302, doi:10.1029/2003JD004255.

Randel, W. J., F. Wu, S. J. Oltmans, K. Rosenlof, and G. E. Nedoluha (2004), Interannual changes of stratospheric water vapour and correlations with tropical tropopause temperatures, *J. Atmos. Sci.*, *61*, 2133–2148.

Sokolik, I. N. (2002), The spectral radiative signature of wind-blown mineral dust: Implications for remote sensing in the thermal IR region, *Geophys. Res. Lett.*, *29*(24), 2154, doi:10.1029/2002GL015910.

Stephens, G. L., S. C. Tsay, P. W. Stackhouse Jr., and P. J. Flateau (1990), The relevance of the microphysical and radiative properties of cirrus clouds to the climate and climatic feedback, *J. Atmos. Sci.*, *47*, 1742–1753.

Tian, B., B. J. Soden, and X. Wu (2004), Diurnal cycle of convection, clouds, and water vapour in the tropical upper troposphere: Satellites versus general circulation model, *J. Geophys. Res.*, *109*, D10101, doi:10.1029/2003JD004117.

Toon, O. W., M. A. Tolbert, B. G. Koehler, M. Middlebrook, and J. Jordan (1994), Infrared optical constants of H_2O ice, amorphous nitric acid solutions, and nitric acid hydrates, *J. Geophys. Res.*, *99*, 25,631–25,654.

Voigt, C., et al. (2000), Nitric acid trihydrate (NAT) in polar stratospheric cloud particles, *Science*, *290*, 1756–1758.

von Kuhlmann, R., and M. G. Lawrence (2005), The impact of ice uptake of nitric acid on atmospheric chemistry, *Atmos. Chem. Phys. Disc.*, *5*, 7361–7386.

Williams, E., K. Rothkin, D. Stevenson, and D. Boccippio (2000), Global lightning variations caused by changes in thunderstorms flash rate and by changes in the number of thunderstorms, *J. Appl. Meteorol.*, *39*, 2223–2230.

Wornsop, D. R., L. E. Fox, M. S. Zahniser, and S. C. Wosfy (1993), Vapor pressures of solid hydrates of nitric acid: Implications for polar stratospheric clouds, *Science*, *259*, 71–74.

Zhou, X., M. A. Geller, and M. Zhang (2004), Temperature fields in the tropical tropopause transition layer, *J. Clim.*, *17*, 2901–2908.

H. Chepfer and M. Chiriaco, Laboratoire de Météorologie Dynamique/Institut Pierre-Simon Laplace, Ecole Polytechnique, Route de Saclay, F-91128 Palaiseau Cedex, France. (chepfer@lmd.polytechnique.fr)

P. Dubuisson, Laboratoire Écosystèmes Littoraux et Côtiers, Université du Littoral, F-62930 Wimereux, France.

P. Minnis, NASA Langley Research Center, Hampton, VA 23681, USA.

E. D. Rivière, Laboratoire de Physique et Chimie de l'Environnement, Centre National de la Recherche Scientifique/Université d'Orléans, F-45071 Orléans, France.

S. Sun-Mack, Science Applications International Corporation, Hampton, VA 23666, USA.